

COB-2023-1859

HEURISTIC OPTIMIZATION METHODOLOGY APPLIED TO PASSIVE VIBRATION CONTROL USING CONSTRAINED LAYERS ON PLATES

Sandmara Lanhi

Luiz Otávio Rigobello Muraro

Jucélio Tomás Pereira

Federal University of Paraná, Polytechnic Center, 100 Cel. Francisco H. dos Santos, Curitiba PR 81530-000

sandmara_lanhi@hotmail.com; luizotavorigobello@gmail.com; jucelio.tomas@ufpr.br

Abstract. *Metallic plates and shells are structural elements that provide support for static and dynamic loads. They are also the main sources of noise and vibrations. One way to avoid these problems is to use passive vibration control through constrained layers (CLs). Typically, only a portion of the primary system area is covered by the CL to avoid excessive increases in mass and cost. Many optimization methods are employed to determine the optimal CL distribution. However, most optimization methods used require a lot of computational time to determine an optimum, even if it is not a global optimum. In addition, topological optimization methods based on finite elements can lead to the appearance of checkerboards. In this context, this work aims to present a heuristic topology optimization methodology, applied to the passive control of plate vibration using CL. The objective is to present a simple and efficient heuristic methodology that obtains good results for controlling vibrations in plates and that can minimize checkerboard effects. The evaluated objective function is the Euclidean norm of a component of the matrix inertance function, while the design variables correspond to the positions of the CLs. As results, the plate vibration control for the first four modes individually, the vibration control of two and for modes are presented.*

Keywords: *viscoelastic material, finite element method, plates, topology optimization.*

1. INTRODUCTION

Metallic plates and shells are structural elements responsible for supporting static and dynamic loads in cars, ships, planes, and aerospace vehicles. They are also the main source of noise and vibration due to their low damping, low stiffness, and wide sound radiation surface (Zheng *et al.*, 2016). Frequently, the passive vibration control by constrained layer (CL) can be considered an effective and robust technique to reduce vibration levels in plates and shells (Zhang *et al.*, 2022). Furthermore, CLs are known for their ease of application and maintenance. They exhibit high damping ratios over a wide range of frequencies and temperatures.

The constrained layer is constituted by a layer of viscoelastic material (VEM) superimposed, usually by a layer of metallic material, called the constraining layer. The CL is placed over the primary system, which is the system that needs to be controlled (Kudal and Cicirello, 2018; Wang *et al.*, 2021). The dissipation of vibrational energy occurs through the shear deformation of viscoelastic material (VEM), due to the difference in displacements between the primary system and the constraining layer (Madeira *et al.*, 2020; Chen *et al.*, 2021).

In practice, only a percentage of the outer surface of the primary system is covered with CL. This is usually done to avoid a significant increase in weight and cost. In this sense, considering only a percentage of the area covered by CL, it is necessary to optimize the positioning of the CL to achieve the best efficiency in vibration control in a given frequency range. Several works suggest different CL optimization formulations, including topological optimization (Ling *et al.*, 2011; Chen *et al.*, 2021; Xu *et al.*, 2021; Zhang *et al.*, 2021; Cui *et al.*, 2022).

However, the cited optimization methods may require a very high computational effort to find an optimal solution. In this sense, this work aims to present a simple and efficient heuristic topology optimization methodology applied to the passive vibration control of plates using CL. The proposed methodology consists of performing a finite element analysis and obtaining the dynamic response of the structure by adding CL individually to each FE. So, it is possible to evaluate the effect of including CL in a single FE in reducing the dynamic response of the entire structure, classifying them by effectiveness. In a subsequent step, a percentage of the best elements is chosen to cover the plate. Then, the dynamic response of the system is evaluated again, adding CL individually to the other FEs. This process is repeated until a maximum percentage coverage area is reached. The efficiency of each element is evaluated by the difference between the Euclidean norm of the inertance function of the primary system, with the Euclidean norm of the inertance function of the damped system. The methodology was implemented in the MATLAB software.

2. VISCOELASTIC MATERIALS

Viscoelastic materials (VEMs) are used in several areas such as automotive, space, aeronautics and military. The main reason for its wide use is its ability to dissipate vibrational energy and noise. A principal aspect of these materials is that their properties can vary significantly with frequency and temperature (Mainardi, 2022). A mathematical model used to describe the relationship between the temperature and the frequency is the shift factor of Williams-Landel-Ferry (WLF) (Gutierrez-Lemini, 2014). The shift factor can be obtained by the equation

$$\log_{10}\alpha_T = -\frac{\theta_1(T - T_0)}{\theta_2 + (T - T_0)}, \quad (1)$$

where θ_1 and θ_2 are material parameters obtained experimentally, T_0 is the reference temperature and T is the VEM working temperature. The equation that relates the shift factor, α_T , to the temperature and working frequency is

$$\Omega_r = \alpha_T \Omega, \quad (2)$$

where Ω_r is the reduced frequency.

Using the constitutive model of fractional Zener derivatives (Findley and Davis, 2013; Mainardi, 2022) the complex modulus of elasticity to VEM can be described according to the equation

$$E_c(\Omega) = \frac{E_0 + E_\infty \phi_0 (i\Omega_r)^\beta}{1 + \phi_0 (i\Omega_r)^\beta}, \quad (3)$$

where E_0 , E_∞ , ϕ_0 and β are parameters of the VEM obtained experimentally. E_0 and E_∞ are asymptotic values of the real part of $E_c(\Omega)$ when Ω tends to zero and Ω tends to infinite, respectively. β is the order of the fractional derivative and $\phi_0 = b_0^\beta$ is a constant associated with the relaxation time of the material, and b_0 is computed at the reference temperature T_0 .

3. HEURISTICS METHODS FOR OPTIMIZATION

Heuristic optimization methods aim to obtain good solutions (not necessarily optimal) for difficult and complex problems through simple, easy, and fast procedures (Zanakis and Evans, 1981). One of the main reasons for using these methods is that, generally, the methods that guarantee an optimal solution are computationally less attractive due to excessive processing time. Furthermore, in complex problems, it may be difficult to find an optimal solution even with large computational efforts. On the other hand, heuristic methods offer the advantage of providing feasible solutions in a short period of time (Zanakis and Evans, 1981). Moreover, heuristic methods can provide initial solutions for other optimization methods, thus reducing the number of candidate solutions. Among the heuristic methods for structural optimization, the Evolutionary Structural Optimization (ESO) method stands out (Chu *et al.*, 1996; Huang and Xie, 2010).

3.1 Evolutionary Structural Optimization Method - ESO

The Evolutionary Structural Optimization Method (ESO) consists of the simplified concept of gradually removing inefficient material from a structure, following a specific criterion. The goal of the method is for the shape and topology of the resulting structure to converge to an optimum, not necessarily a global optimum (Chu *et al.*, 1996).

According to EF analysis done on ESO, it is possible to identify the inefficient finite elements. In the originally proposed method, a finite element is inefficient if your effective stress is low, for example. This concept leads to a rejection criterion based on the local stress level of the structure, where the elements with low stress are considered underutilized and can therefore be removed (Huang and Xie, 2010). Based on this, the stress level in each element is calculated using the effective element failure stress (σ_e), which is compared to the maximum effective failure stress of the entire structure (σ_{max}). Then, the elements that do not satisfy the relation

$$\frac{\sigma_e}{\sigma_{max}} < RR_i, \quad (4)$$

are removed from structure. In this equation, RR_i is the current rejection ratio. The process of finite element analysis and removal of inefficient elements is carried out until an optimum is achieved, for example, when there is no longer any material in the structure with a stress level below 30% of the maximum value (Huang and Xie, 2010).

3.2 Heuristic method for CL optimization

The optimization methodology that we developed and presented in this work is based on a heuristic methodology that uses the calculation of the Euclidean norm of the inertance function ($A_{ks}(\Omega)$). We defined this function as the objective

function (Eq. 8). The methodology was developed and applied in the analysis of vibrations in plates with passive vibration control by CL. Our objective is to obtain near-optimal results in an efficient and fast way. The methodology consists of evaluating the modification of the objective function value when each FE receives CL separately, classification of the best FEs, and coverage the primary system by CL in a specific percentage.

The structure of the primary system was discretized in n_{el} finite elements. In each covering of the EF separately, the FE analysis was performed taking into account the dynamic excitation and the boundary conditions of the structure. In this way, it was possible to obtain an approximation of the Euclidean norm of the inertance function of the primary system, denoted by $A_{kssp}(\Omega)$.

Subsequently, CL is attached to each FE individually, and the objective function is calculated for each configuration ($A_{ks(i)}$). With this, it is possible to classify (rank) the EFs based on the value of the objective function, highlighting those that provide the greatest reduction. How much each EF with CL reduces the inertance of the primary system (A_{kssp}) is determined by Eq. (5)

$$M_{(i)} = A_{kssp} - A_{ks(i)}. \quad (5)$$

In a subsequent step, the best elements are selected to cover the plate with CL. The number of selected elements is defined by n_{EAR} . This selection is based on the element addition ratio (EAR), which is set by the user. The objective is to choose the elements that present the greatest reduction in the objective function.

After the initial selection, the CL is assigned to the other mesh elements, one by one, and the ranking is performed again considering only the remaining elements ($n_{el} - n_{EAR}$). This adding and ranking process is repeated until a maximum area (S_{max}) of coverage is reached.

The optimization process can be summarized in the steps presented below:

1. Discretize the primary system in n_{el} finite elements;
2. Perform finite element analysis;
3. Compute the objective function for each FE solely receiving CL;
4. Classify the elements, according to Eq. (5);
5. Assign CL to n_{EAR} elements;
6. Repeat step 2 to 4 until the coverage constraint is satisfied, that is, until S_{max} is reached.

The methodology aims to identify the most effective elements to cover the plate with CL and reduce the objective function. This selection is carried out taking into account criteria established by the user, such as the element addition rate (EAR), control frequency range, excitation degree of freedom, response degree of freedom and system boundary conditions. By using the element addition ratio as a criterion, the methodology allows the user to control the amount of elements that will be added to cover the plate with CL.

The methodology developed in this work follows an inverse process than the method known as ESO. In this methodology, finite elements are selected based on their contribution to the reduction of the objective function. Unlike the ESO, in which ineffective elements are removed for optimization, in this methodology elements that have a greater influence on the reduction of the objective function are added. This approach allows focusing on the most relevant elements for obtaining best results. However, it is important to note that both the element addition ratio and the maximum percentage of plate coverage by CL are defined by the user. This ensures that the user can adjust the complexity and performance of the passive vibration control system to their specific needs and constraints.

4. METHODOLOGY

The methodology developed in this work uses concepts of heuristic optimization based on the approximation of the Euclidean norm of the inertance function in the control of vibrations in plates using CL.

4.1 Optimization problem

The plate is discretized into n_{el} finite elements, which each FE corresponding to a design variable. The size of the vector of design variables is equal a n_{el} . Besides that, the vector of design variables is a vector of binary numbers ($\{\mathbf{x}^{(i)} \in \{0, 1\} | i = 1, \dots, n_{el}\}$), where a value equal to 0 means that the element does not contain CL, and a value equal to 1 corresponds to the presence of CL. Figure 1 represents the relation between the design variables with the finite element mesh.

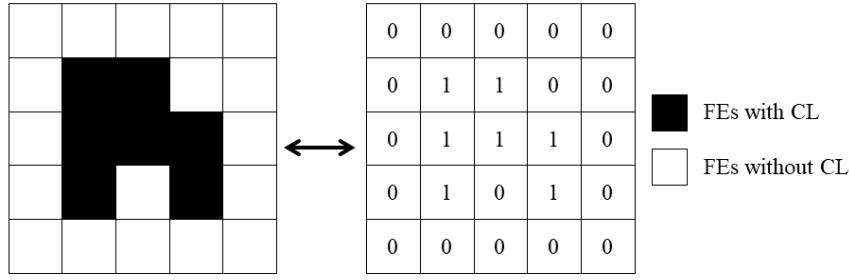


Figure 1. Relation of design variables with mesh elements.

The problem to be solved in this work is a vibration problem, for which the equation of motion (in the frequency domain) needs to be solved

$$([K(\Omega)] - \Omega^2[M])\{X(\Omega)\} = \{F(\Omega)\}, \quad (6)$$

where $[M]$ is the system global mass matrix, $X(\Omega)$ is the generalized displacement response vector, $F(\Omega)$ is the excitation vector (generalized forces vector) and $[K(\Omega)]$ is the system global stiffness matrix, composed of complex and frequency-dependent terms. This matrix can be divided between the purely elastic term $[K_e]$ and the viscoelastic portion $[K_v(\Omega)]$, given as

$$[K(\Omega)] = [K_e] + [K_v(\Omega)]. \quad (7)$$

The elastic portion ($[K_e]$) is composed of real and constant terms, while the viscoelastic portion $[K_v(\Omega)]$ is composed of complex values that are dependent on frequency and temperature.

The solution of Eq. (6) involves frequency-dependent parameters, requiring the discretization of this variable within the analyzed interval. In the case of a "modal analysis-based solution," this step is necessary because these parameters do not allow for the decoupling of the equations due to a nonlinear eigenvalue/eigenvector problem. Thus, two approaches to finding the solution are possible. The first involves solving n linear systems of equations, each system being solved for a discrete value of frequency. The second way is solving an eigenvalues/eigenvectors problem associated with Eq. (6). Both methods require high computational time. Therefore, a method that has been used and presents fast results is the method developed by Floody *et al.* (2007) which we used in this work.

The objective function used in this work is an approximation of the L_2 -norm of a given component ks of the inertance matrix, in the form

$$f(\{x\}) = \frac{\Delta\Omega}{n_i} \sum_{k=1}^{n_i} |A_{ks}(\Omega)|^2 \quad (8)$$

being that $\Delta\Omega = \Omega_f - \Omega_i$, with Ω_i and Ω_f are the values of the initial and final frequencies that limit the frequency range of interest and n_i the number of inertance values sampled in this range. In turn, the inertance, A_{ks} , is the relation between the acceleration ($-\Omega^2 X_k(\Omega)$) measured in one degree of freedom k and the excitation force ($F_s(\Omega)$) applied at the degree of freedom s , given by the equation

$$A_{ks}(\Omega) = -\frac{\Omega^2 X_k(\Omega)}{F_s(\Omega)}. \quad (9)$$

The structure is not fully covered by CL. Thus, a restriction ($g(\mathbf{x})$) is applied to the optimization problem that limits the total area of maximum coverage (S_{max}) of the plate. Considering the constraint, the optimization problem can be written in its standard form as:

$$\begin{aligned} \min \quad & f(\{x\}) = \frac{\Delta\Omega}{n_i} \sum_{k=1}^{n_i} |A_{ks}(\Omega)|^2 \\ \text{s.t.} \quad & g(\{x\}) = \sum_{q=1}^{n_{el}} x_q S_q - S_{max} \leq 0 \end{aligned} \quad (10)$$

where S_q is the surface area of q -th FE.

4.2 Geometry and material properties

The base plate has length, width and thickness values equal to 450 mm, 180 mm and 9 mm, respectively. Both base plate and constraining layer are ASTM-A36 steel with modulus of elasticity equal to 200 GPa, Poisson coefficient equal to 0.3 and density equal to 7860 kg/m³. The thickness of the constraining layer is 1 mm and the thickness of the VEM layer is 5.48 mm.

The physical parameters that characterize the mechanical properties of VEM were obtained from the nomograms of the materials, through numerical methodology based on the fractional Zener model developed by Sousa *et al.* (2017). The viscoelastic material used is EAR C-2003 with the mechanical properties shown in Table 1 (Silva (2019)).

Table 1. Parameters of the viscoelastic material - EAR C-2003

T_0 (K)	T (K)	E_0 (Pa)	E_∞ (Pa)	β	ϕ_0 (b_0^β)	θ_1	θ_2 (K)	ρ (kg/m ³)	ν
314.9	291.15	7.11E+06	9.63E+09	0.479	1.6E-03	126.49	1157.0	1714.0	0.49

The plate was discretized into 128 equal elements. The FE used is an isoparametric element of Reissner-Mindlin layerwise plate, which the theory was developed by Moreira *et al.* (2006). The FE has 4 nodes with 9 degrees of freedom each. This element proved to be efficient in capturing the shear behavior of the VEM.

5. DISCUSSION AND RESULTS

All results were obtained considering a plate in free condition. For obtaining the inertance (FRF), we used a unit force vertical force applied at the left-upper node (excitation node), and response (inertance) was obtained at the left-lower node (response node), which are node 1 and node 153, respectively (Fig. 3-8). An addition ratio of 5% CL was used until a maximum coverage of 30% was achieved. The first four modes of vibration of a free plate are illustrated in Fig. 2, together with the corresponding natural frequencies.

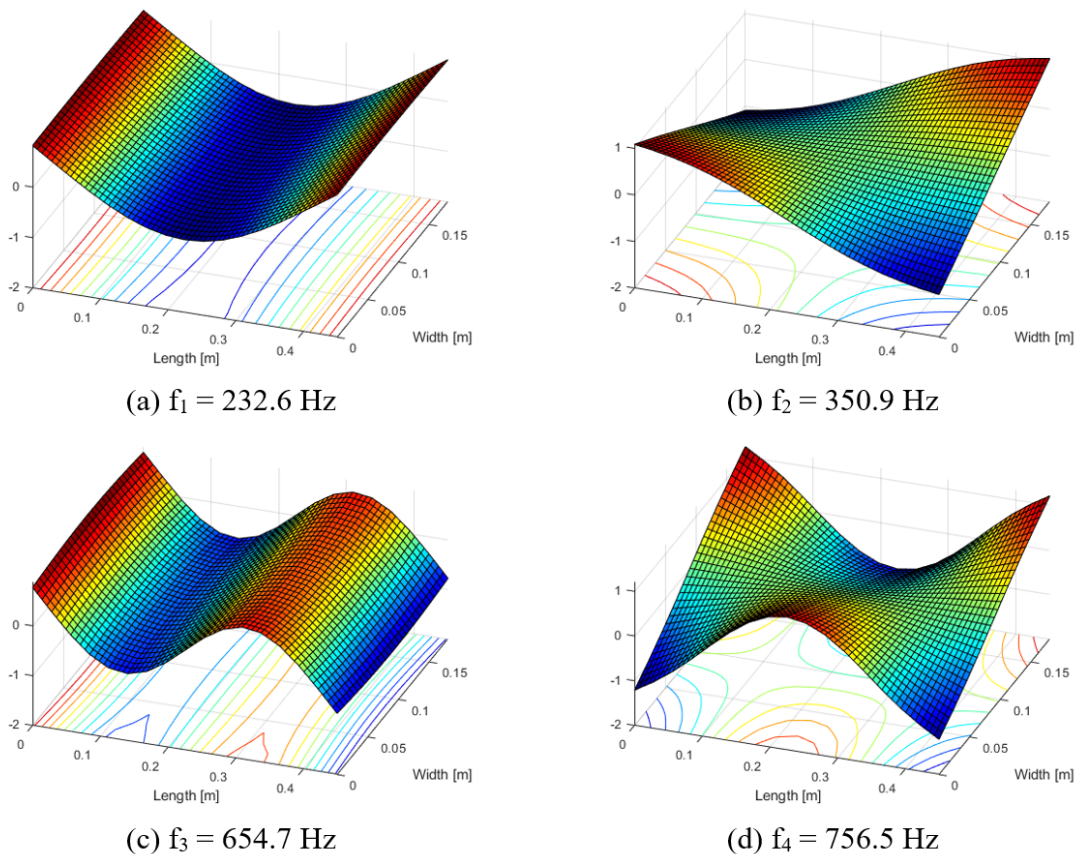


Figure 2. Modes of bending vibration of a free plate.

5.1 Control from the first to fourth mode individually

Passive vibration control by CL was applied to each of the four vibration modes individually. The frequency range that includes the first to four modes is 0 to 1000 Hz, and the natural frequency of the first mode is $f_1 = 232.6$ Hz, of the second mode $f_2 = 350.9$ Hz, of the third mode $f_3 = 654.7$ Hz and of the fourth mode $f_4 = 756.5$

The CL optimal configurations obtained and the respective FRF (frequency response function) are shown in Fig. 3, Fig. 4, Fig. 5 and Fig. 6.

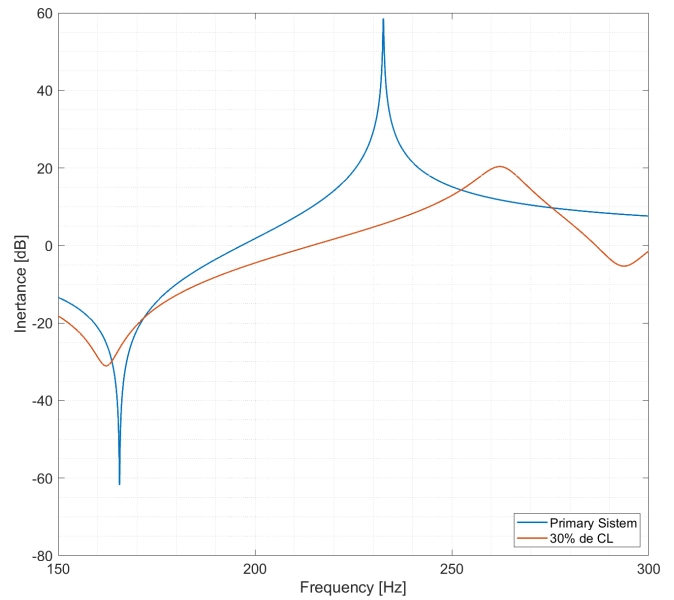
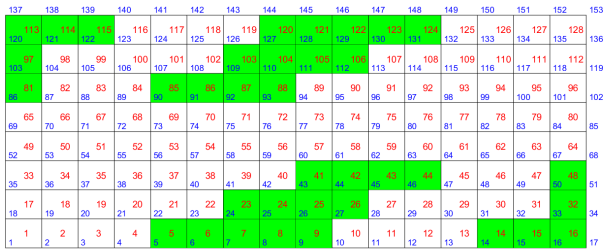


Figure 3. Optimal solution with 30% CL coverage and optimal FRF for the first vibrating mode for a free plate.

In all cases, there is a reduction of about 35 dB in the peak inertance evaluated in the mode of interest, which can be considered highly satisfactory. However, it is important to point out that in our results the placement of the CL may not have been made in the regions of greatest deformation of the structure. This can be attributed to the fact that, when adding CL in small amounts, a modification of the primary system properties, such as mass and stiffness, can occur. Besides that, there is the occurrence of checkerboard in optimal configurations. The checkerboard phenomenon is a numerical instability caused by the use of topological optimization based on FEs. This phenomenon can have an artificially high stiffness and is also difficult to manufacture (Diaz and Sigmund, 1995; Jog and Haber, 1996). To avoid the checkerboard several techniques can be applied ((Diaz and Sigmund, 1995; Jog and Haber, 1996; Fernandes *et al.*, 1999; Jog, 2002)).

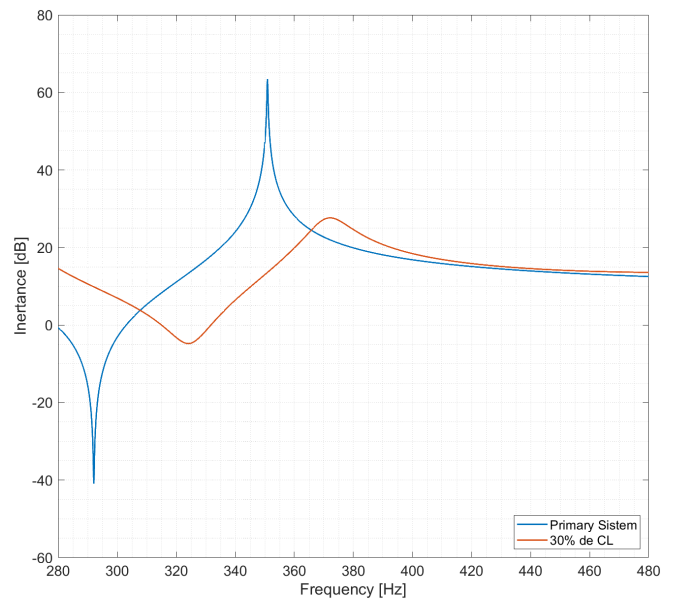
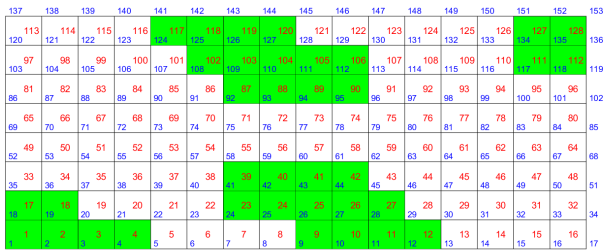


Figure 4. Optimal solution with 30% CL coverage and optimal FRF for the second vibrating mode for a free plate.

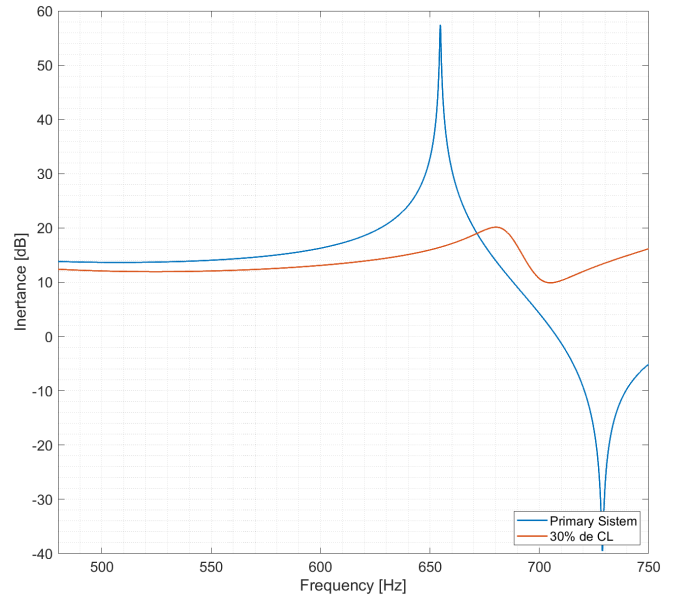
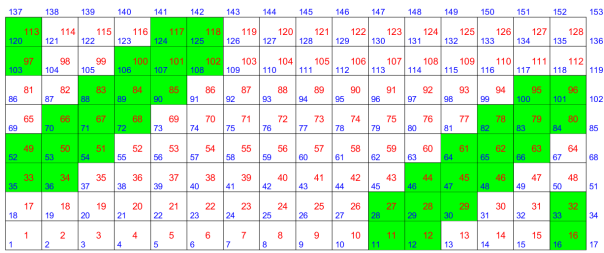


Figure 5. Optimal solution with 30% CL coverage and optimal FRF for the third vibrating mode for a free plate.

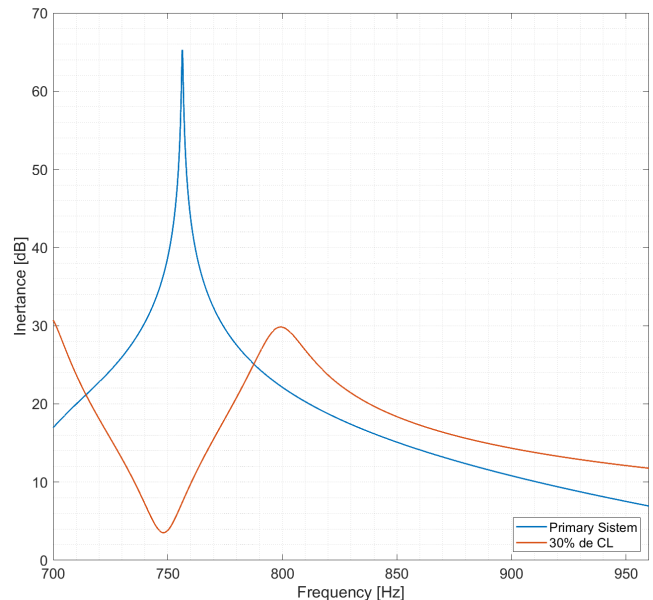


Figure 6. Optimal solution with 30% CL coverage and optimal FRF for the fourth vibrating mode for a free plate.

5.2 Wideband frequency control

In this section, two cases are analyzed. In the first case the first and second vibration modes are evaluated simultaneously. This result was obtained for the same structure evaluated in the previous section, a rectangular plate with free-type Dirichlet boundary conditions. The control comprises a frequency range from 150 to 500 Hz. The optimal CLs configuration obtained is shown in Fig. 7.

Finally, the last case analyzed was the simultaneous control of the four vibration modes, which lie in the frequency range from 0 to 900 Hz. The optimal CL distribution and the corresponding FFR are presented in Fig. 8. The two results presented in this subsection show effective control of all modes comprised by the analyzed frequency range. In addition, they present a reduction of more than 30 dB in peak inertance values.

6. CONCLUSIONS

This work presents a simple and efficient methodology to obtain the optimal distribution of CL (constrained layer) on a metallic plate under free condition. The approach utilizes concepts of heuristic optimization and approximates the L_2 -norm of the inertance function.

The methodology has demonstrated effectiveness in both narrowband and broadband frequency control. For narrow-

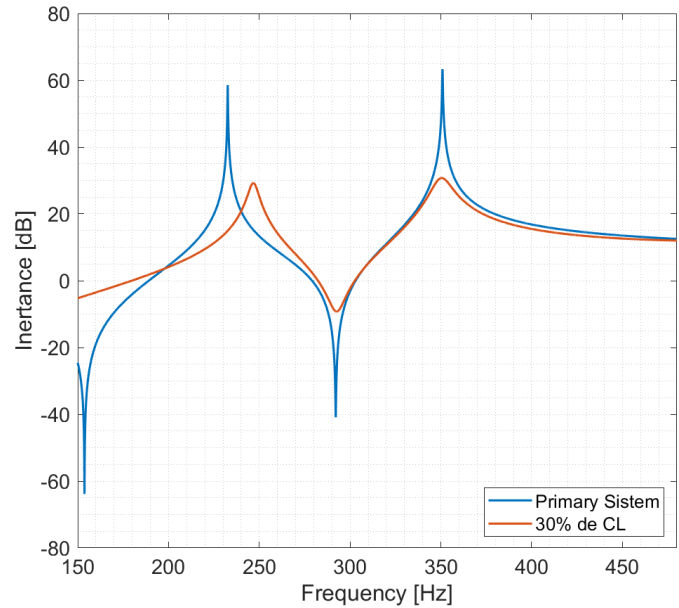
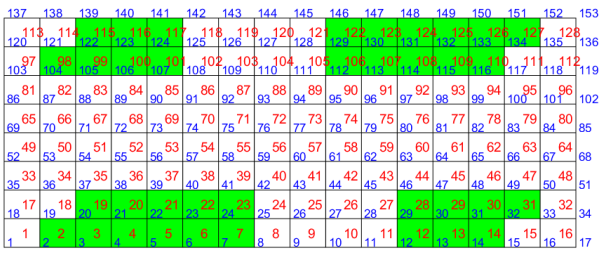


Figure 7. Optimal solution with 30% CL coverage and optimal FRF for the first and second vibration mode for a free plate.

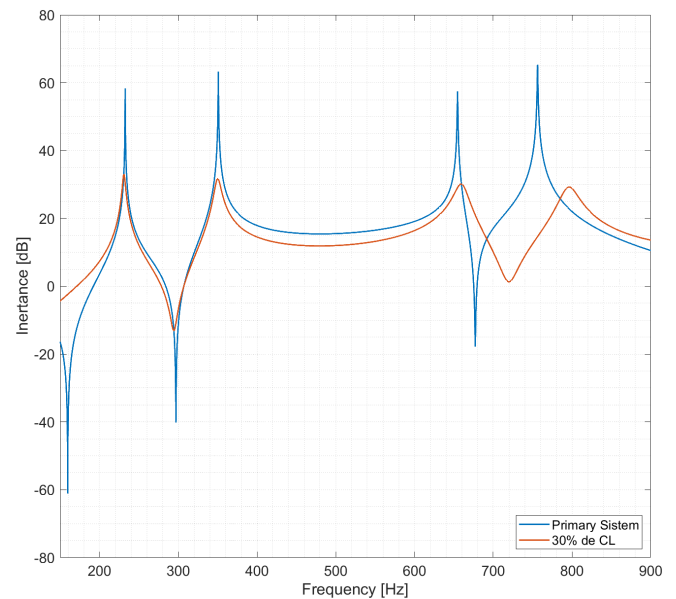
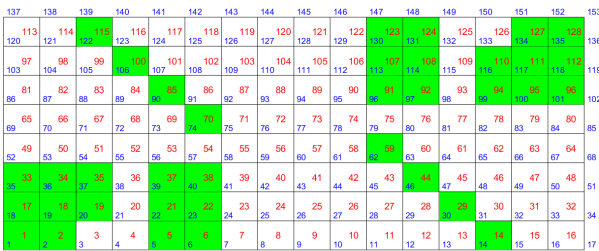


Figure 8. Optimal solution with 30% CL coverage controlling from the first to the fourth mode for a free plate.

band frequency control, the four lowest modes were individually analyzed. As for broadband control, two modes were initially controlled, followed by four modes. In both cases, a reduction of approximately 30 dB in the inertance peak was observed.

However, despite the satisfactory results, the phenomenon of checkerboard was identified in some cases. This phenomenon can occur in topology optimization methods based on finite element method, as in this work. The solid-void pattern generated by checkerboard can result in artificially increased stiffness and pose challenges in manufacturing. Therefore, it is necessary to find ways to avoid this phenomenon.

7. ACKNOWLEDGEMENTS

The authors thank the Post-Graduated Program in Mechanical Engineering (PG-Mec) from Federal University of Paraná (UFPR), Brazil. Furthermore, Sandmara Lanhi would like to acknowledge the Programa de Recursos Humanos da Agência Nacional de Petróleo, Gás Natural e Biocombustíveis (PRH-ANP) and Luiz Otávio Rigobello Muraro would like to thank the Coordenação de Aperfeiçoamento de Pessoal de Nível Superior (CAPES) for their financial support.

8. REFERENCES

- Chen, R., Luo, H., Wang, H. and Zhou, W., 2021. "Topology optimization of partial constrained layer damping treatment on plate for maximizing modal loss factors". *Composites and Advanced Materials*, Vol. 30, pp. 1–19.
- Chu, D.N., Xie, Y., Hira, A. and Steven, G., 1996. "Evolutionary structural optimization for problems with stiffness constraints". *Finite elements in analysis and design*, Vol. 21, No. 4, pp. 239–251.
- Cui, M., Wang, J., Li, P. and Pan, M., 2022. "Topology optimization of plates with constrained layer damping treatments using a modified guide-weight method". *Journal of Vibration Engineering & Technologies*, pp. 1–18.
- Diaz, A. and Sigmund, O., 1995. "Checkerboard patterns in layout optimization". *Structural optimization*, Vol. 10, pp. 40–45.
- Fernandes, P., Guedes, J.M. and Rodrigues, H., 1999. "Topology optimization of three-dimensional linear elastic structures with a constraint on "perimeter"". *Computers & Structures*, Vol. 73, No. 6, pp. 583–594.
- Findley, W.N. and Davis, F.A., 2013. *Creep and relaxation of nonlinear viscoelastic materials*. Courier corporation.
- Floody, S.E., Arenas, J.P. and De Espindola, J.J., 2007. "Modelling metal-elastomer composite structures using a finite-element-method approach". *Strojnicki Vestnik*, Vol. 53, No. 2, pp. 66–77.
- Gutierrez-Lemini, D., 2014. *Engineering viscoelasticity*. Springer.
- Huang, X. and Xie, M., 2010. *Evolutionary topology optimization of continuum structures: methods and applications*. John Wiley & Sons.
- Jog, C.S. and Haber, R.B., 1996. "Stability of finite element models for distributed-parameter optimization and topology design". *Computer methods in applied mechanics and engineering*, Vol. 130, No. 3-4, pp. 203–226.
- Jog, C., 2002. "Topology design of structures using a dual algorithm and a constraint on the perimeter". *International Journal for Numerical Methods in Engineering*, Vol. 54, No. 7, pp. 1007–1019.
- Kudal, A. and Cicirello, A., 2018. "Constrained layer damping treatment: Analysis of multi-strip application on thin plates". In *Journal of Physics: Conference Series*. IOP Publishing, p. 012025.
- Ling, Z., Ronglu, X., Yi, W. and El-Sabbagh, A., 2011. "Topology optimization of constrained layer damping on plates using method of moving asymptote (mma) approach". *Shock and Vibration*, Vol. 18, pp. 221–244.
- Madeira, J., Araújo, A.L., Soares, C.M. and Soares, C.M., 2020. "Multiobjective optimization for vibration reduction in composite plate structures using constrained layer damping". *Computers & Structures*, Vol. 232, p. 105810.
- Mainardi, F., 2022. *Fractional calculus and waves in linear viscoelasticity: an introduction to mathematical models*. World Scientific.
- Moreira, R., Rodrigues, J.D. and Ferreira, A., 2006. "A generalized layerwise finite element for multi-layer damping treatments". *Computational Mechanics*, Vol. 37, pp. 426–444.
- Silva, F.E.C., 2019. *Projeto ótimo de neutralizadores dinâmicos com múltiplos graus de liberdade considerando os parâmetros físicos, localização e material viscoelástico (in Portuguese)*. Master's thesis, Graduate Program in Mechanical Engineering, Federal University of Paraná, Curitiba, Brasil.
- Sousa, T.L., Kanke, F., Pereira, J.T. and Bavastrri, C.A., 2017. "Property identification of viscoelastic solid materials in nomograms using optimization techniques". *Journal of Theoretical and Applied Mechanics*, Vol. 55, No. 4, pp. 1285–1297.
- Wang, H., Lee, H.P. and Du, C., 2021. "Analysis and optimization of damping properties of constrained layer damping structures with multilayers". *Shock and Vibration*, Vol. 2021, pp. 1–11.
- Xu, K., Chen, Z. and Sun, W., 2021. "Optimization of position, size and thickness of viscoelastic damping patch for vibration reduction of a cylindrical shell structure". *Composite Structures*, Vol. 276, p. 114573.
- Zanakis, S.H. and Evans, J.R., 1981. "Heuristic "optimization": Why, when, and how to use it". *Interfaces*, Vol. 11, No. 5, pp. 84–91.
- Zhang, D., Wu, Y., Lu, X. and Zheng, L., 2022. *Mechanics of Advanced Materials and Structures*, Vol. 29, pp. 154–170.
- Zhang, J., Chen, Y., Zhai, J., Hou, Z. and Han, Q., 2021. "Topological optimization design on constrained layer damping treatment for vibration suppression of aircraft panel via improved evolutionary structural optimization". *Aerospace Science and Technology*, Vol. 112, p. 106619.
- Zheng, W., Yang, T., Huang, Q. and He, Z., 2016. "Topology optimization of PCLD on plates for minimizing sound radiation at low frequency resonance". *Structural and Multidisciplinary Optimization*, Vol. 53, pp. 1231–1242.

9. RESPONSIBILITY NOTICE

The authors are solely responsible for the printed material included in this paper.